RARE METALS

ORIGINAL ARTICLE

Layer-dependent and light-tunable surface potential of two-dimensional indium selenide (InSe) flakes

Yu-Hao Li, Chuang-Bin Yu, Zhi Li, Peng Jiang, Xiao-Yuan Zhou* ,
Cun-Fa Gao*, Jiang-Yu Li*

Abstract As a fundamental surface property of two-dimensional (2D) materials, surface potential is critical for their emerging electronic applications and essential for van der Waals heterostructure engineering. Here, we report the surface potential of few-layer InSe. The effect of layer count, light intensity and different deposited substrates is considered. Few-layer InSe flakes were exfoliated from bulk InSe crystals on Si/SiO_2 with 300-nm-thick thermal oxide and Si/SiO_2 with 300-nm-thick thermal oxide and prefabricated micro-wells with 3 μm in diameter. The samples were measured by Kelvin probe force microscopy and tuned by an integrated 405-nm (3.06 eV) laser. Based on the work function of SiO_2 (5.00 eV), the work functions of supported and suspended InSe are determined. These results show that the work function of InSe decreases with the increase in the layer count of both supported InSe and suspended InSe. Besides, by introducing a tunable laser light, the influence of light intensity on surface potential of supported InSe was studied. The surface potential (SP) and surface potential shift between light and dark states ($\Delta SP = SP_{light} - SP_{dark}$) of supported InSe were measured and determined. These results present that the surface potential of supported InSe decreases with the increase in the light intensity and also decreases with the increase in the layer count. This is evident that light excites electrons, resulting in decreased surface potential, and the amount of electrons excited is correlated with light intensity. Meanwhile, ΔSP between light and dark states decreases with the increase in the layer count, which suggests that the influence of light illumination decreases with the increase in the layer count of few-layer InSe flakes.

Keywords Indium selenide (InSe); Kelvin probe force microscopy; Surface potential; Work function

Y.-H. Li, C.-B. Yu, Z. Li, C.-F. Gao*
State Key Laboratory of Mechanics and Control of Mechanical Structures, Nanjing University of Aeronautics and Astronautics, Nanjing 210016, China
e-mail: cfgao@nuaa.edu.cn

Y.-H. Li, Z. Li, P. Jiang, X.-Y. Zhou*, J.-Y. Li*
Shenzhen Key Laboratory of Nanobiomechanics, Shenzhen Institutes of Advanced Technology, Chinese Academy of Sciences, Shenzhen 518055, China
e-mail: xiaoyuan2013@cqu.edu.cn

J.-Y. Li
e-mail: jy.li1@siat.ac.cn

Y.-H. Li
Department of Physics, University of Washington, Seattle, WA 98195, USA

X.-Y. Zhou
Department of Applied Physics, State Key Laboratory of Power Transmission Equipment and System Security and New Technology, Chongqing University, Chongqing 400044, China

1 Introduction

Two-dimensional (2D) materials, such as graphene [1] and group III chalcogenides [2], have become worldwide research hot spots due to its advanced functional properties that can be useful for a wide range of applications [3–5]. What the most interested is the electric properties of 2D materials that have high carrier mobility under low temperature; such unusual combination opens exciting opportunities for their emerging applications in electronics and photonics [6]. The atomic thin graphene [7] combined with atomically smooth surface substrate [8] and edge-contact geometry [9] makes the electric properties of crystal

approach its theoretical phonon-scattering limit. The surface potential of 2D material is related to its Fermi level, which is vital to its electric properties, such as the contact barriers and carrier concentration, so the surface potential of 2D material is crucial for the booming van der Waals heterostructure engineering that aligns the 2D material surfaces one by one vertically [10].

Indium selenide (InSe) is a member of layered group III chalcogenide semiconductors [11]. Recent study shows that 2D electron gas induced by the field effect on the surface of few-layer InSe showed high carrier mobility up to 1×10^3 and 1×10^4 cm$^2 \cdot$V$^{-1} \cdot$s^{-1} at room and liquid helium temperatures [12], respectively, accompanying with fully developed quantum Hall effect. The few-layer InSe also shows impressive high Young's modulus and intrinsic strength of 101.73 and 8.68 GPa [13], respectively. Meanwhile, black phosphorous/InSe-based photodetector shows fast response ($\sim$ 22 ms) and high responsivity for visible and near-infrared light [14]. However, the surface potential of few-layer InSe still lacks attention due to its air sensitivity and researcher's partiality on other 2D materials, especially for MoS_2 [15]. The surface potential and work function of MoS_2 are well understood, and researchers explored the effect of factors of surface potential such as layer count, light intensity, electric bias, methods of sample preparation and different substrates [16–19]. Mechanisms for the change of work function of MoS_2 were also proposed, such as interlayer screening effects [16], the adsorption of water/oxygen molecules [17] and charge distribution [18]. For InSe, the theoretical study on work function of InSe was very recently proposed based on density functional theory, presenting that the work function of InSe decreases from 5.22 to 4.77 eV when the InSe stacks together from monolayer to bulk [20]. And the experimental study for the surface potential of few-layer InSe is still absent.

Here, the exfoliated few-layer InSe was studied by Kelvin probe force microscopy (KPFM) [21, 22]. Firstly, few-layer InSe flakes were exfoliated from bulk InSe crystals and on Si/SiO$_2$ with 300-nm-thick thermal oxide (supported InSe) and Si/SiO$_2$ with 300-nm-thick thermal oxide and prefabricated micro-wells with 3 μm in diameter (suspended InSe). Then, the surface potential of InSe flakes was measured by KPFM. To determine the exact value of surface potential, the surface potential maps were divided into several parts based on their layer count, and then, the corresponding work functions were determined by treating SiO$_2$ as a reference. These results show that the work function of InSe decreases with the increase in the layer count of both suspended InSe and supported InSe. By illuminating light, the surface potential (SP) and surface potential shift (ΔSP) between light and dark states of supported InSe were measured and deduced, respectively; these results give the evidence that how the light affects the surface potential of supported InSe, finally.

2 Experimental

2.1 Sample preparation

Few-layer InSe flakes were exfoliated from InSe crystals and on Si/SiO$_2$ with 300-nm-thick thermal oxide and Si/SiO$_2$ with 300-nm-thick thermal oxide and prefabricated micro-wells with 3 μm in diameter. The Scotch tape was used as the transfer medium. More details can be found in our previous works [13, 23, 24]. Specially, due to the instability of InSe in air, all samples were stored in glove box with a nitrogen atmosphere.

2.2 Raman spectroscopy

Raman scattering spectroscopy was performed on a Horiba high-resolution confocal Raman microscope integrated with a 532-nm laser as the excitation source. The characteristic vibrations frequency were used to confirm the optical properties of InSe which is related to its layer count [25]. The LabSpec was used to control the *XYZ* axes motorized sample stage, which can move sample accurately, and the output power was controlled by a series of neutral density filters. Here, a standard D1 (10%) filter was used to attenuate the power intensity of 532-nm laser ($\sim$ 88 mV); as a result, the output power of Raman is less than 9 mW.

2.3 KPFM

Theoretically, by applying an alternating current (AC) voltage ($V_{AC}\sin(\omega t)$) and a direct current (DC) voltage (V_{DC}) to the conductive cantilever, the total voltage applied in tip (V_{tip}) is

$$V_{tip} = V_{DC} + V_{AC}\sin(\omega t) \tag{1}$$

The tip and sample can be modeled as a parallel plate capacitor, and then, the relation between the total potential difference and the electrostatic force (F) can be stated as

$$F = \frac{1}{2}\frac{\partial C}{\partial z}V^2 \tag{2}$$

where C and z are the capacitance and normal distance between tip and sample, respectively; V is the total potential difference between sample and tip, which can be given by

$$V = V_{tip} - V_{SP} = (V_{DC} - V_{SP}) + V_{AC}\sin(\omega t) \quad (3)$$

where V_{SP} is equal to the contact potential difference between cantilever tip and sample, also termed as surface potential (SP) here [22, 26]

$$V_{SP} = \frac{\Phi_{tip} - \Phi_{sample}}{-e} \quad (4)$$

where Φ_{tip} and Φ_{sample} are work function of the tip and sample, respectively, while e is the electric charge carried by a single electron. By inserting Eqs. (3) into (2), the electrostatic force has the form

$$F = \frac{1}{2}\frac{\partial C}{\partial z}[(V_{DC} - V_{SP}) + V_{AC}\sin(\omega t)]^2 = F_{DC} + F_\omega + F_{2\omega} \quad (5)$$

where F_{DC}, F_ω and $F_{2\omega}$ are the DC, ω and 2ω component of force which can be given as

$$F_{DC} = \frac{1}{2}\frac{\partial C}{\partial z}\left[(V_{DC} - V_{SP})^2 + \frac{1}{2}V_{AC}^2\right] \quad (6)$$

$$F_\omega = \frac{\partial C}{\partial z}[(V_{DC} - V_{SP})V_{AC}\sin(\omega t)] \quad (7)$$

$$F_{2\omega} = -\frac{1}{4}\frac{\partial C}{\partial z}V_{AC}^2\cos(2\omega t) \quad (8)$$

From Eq. (7), if we can nullify the ω component of force (F_ω) by adjusting the applied DC voltage, the applied DC voltage (V_{DC}) is equal to the surface potential (V_{SP}). To protect the InSe samples, all KPFM measurements were taken in nitrogen atmosphere.

3 Results and discussion

3.1 A few-layer InSe flake

Monolayer InSe has a honeycomb lattice that consists of four covalently bonded Se–In–In–Se atomic layers, as shown in Fig. 1a, and the layers are held together by vdW interactions with an interlayer distance of $d \approx 0.8$ nm. Few-layer InSe flakes are micro-mechanically exfoliated from bulk InSe crystals and on Si/SiO$_2$ with 300-nm-thick thermal oxidized and Si/SiO$_2$ with 300-nm-thick thermal oxide and prefabricated micro-wells with 3 μm in diameter. The optical image of few-layer InSe on Si/SiO$_2$ is
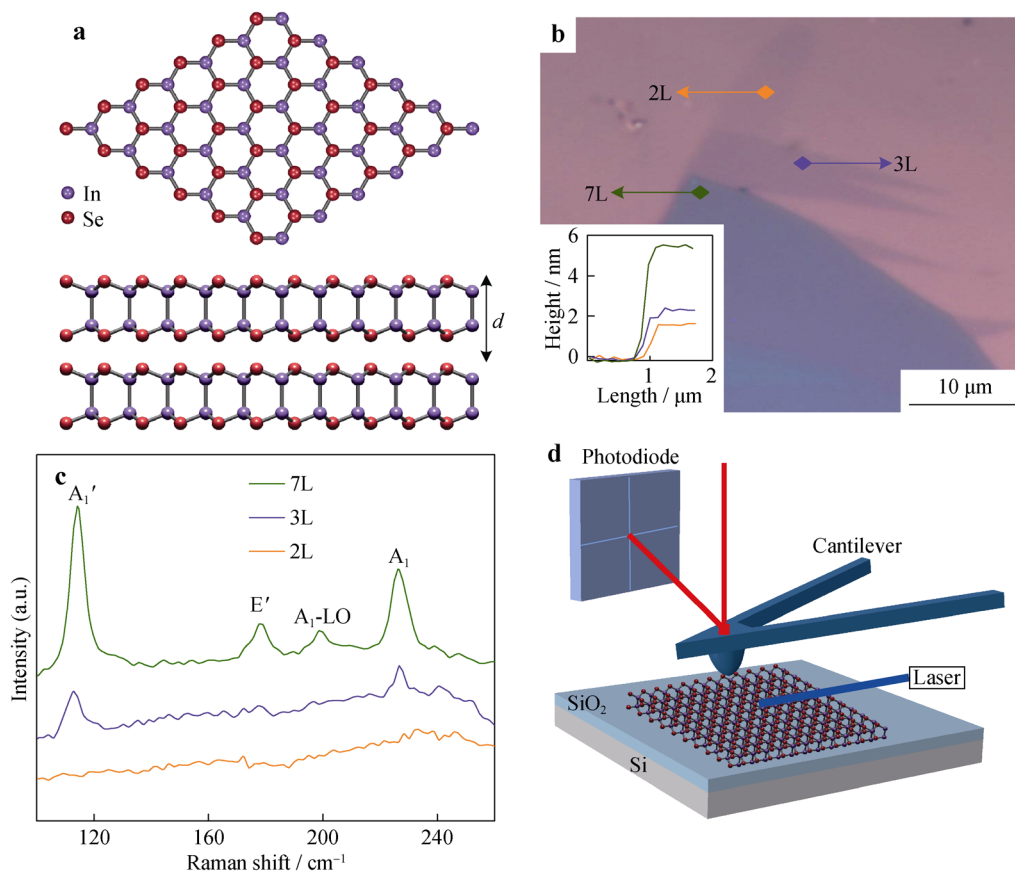

Fig. 1 **a** Crystal structure of InSe; **b** optical image of a few-layer InSe flake deposited on Si/SiO$_2$ and corresponding topography profiles; **c** Raman spectra of 2L, 3L and 7L InSe in range of 100–260 cm^{-1}; **d** schematic of light-excited KPFM

shown in Fig. 1b, wherein few-layer InSe can be judged from their unique optical contrasts [24, 27], and the layer counts were measured by atomic force microscopy (AFM) scans in contact mode, with the resulting topography profiles inserted in Fig. 1b, showing thickness corresponding to 2L, 3L and 7L (L: layers) InSe. The Raman spectra of few-layer InSe are presented in Fig. 1c; four characteristic peaks are observed, which are A_1' (~ 114 cm^{-1}) peak, E' (~ 180 cm^{-1}) peak, A_1-LO (~ 200 cm^{-1}) peak and A_1 (225 cm^{-1}) peak; for 7L InSe, these peaks fade away when the layer count decreases from 7 to 2, which are consistent with the data reported in previous studies [25, 28]. In order to protect the air-sensitive InSe flakes, the samples are stored in glove box with a nitrogen atmosphere. More details of sample preparation and Raman measurement are given in Sect. 2.

3.2 Work function of a few-layer InSe

Work function of 2D materials can be influenced by many factors, including substrate, crystal face and surface contamination. In order to explore the intrinsic work function of InSe, the supported and suspended InSe were prepared, and their work functions were measured by KPFM, as

schematically shown in Fig. 1d. An integrated 405-nm (3.06 eV) laser was also used to excite the samples to study their responses under light illumination. During KPFM measurement, an AC voltage was applied to the scanning tip to produce an oscillation of cantilever, while a DC voltage was applied to suppress such oscillation. Consequently, the applied DC voltage is equal to the contact potential difference between cantilever tip and sample, also termed as surface potential. To prevent degeneration of InSe in air, a steady nitrogen flow was pumped into Cypher ES chamber to maintain a nitrogen atmosphere. More details of KPFM are given in Sect. 2.

Experimentally, Fig. 2a, b presents the topography and surface potential mappings of a few-layer supported InSe from 2L to 7L, and the corresponding results for a few-layer suspended InSe are shown in Fig. 2c, d. Owing to instability of InSe in air, the topography of fresh InSe flake, which is smooth and flat as shown in Fig. 2a, c, is compared with that of degenerated InSe sample which has some bubble-like islands [29], to make sure that the InSe surface is fresh and clean without any degeneration. For supported InSe, it is interesting that the 2L InSe has surface potential (and thus work function) very close to SiO$_2$, this property is different from MoS$_2$ [18] and the surface
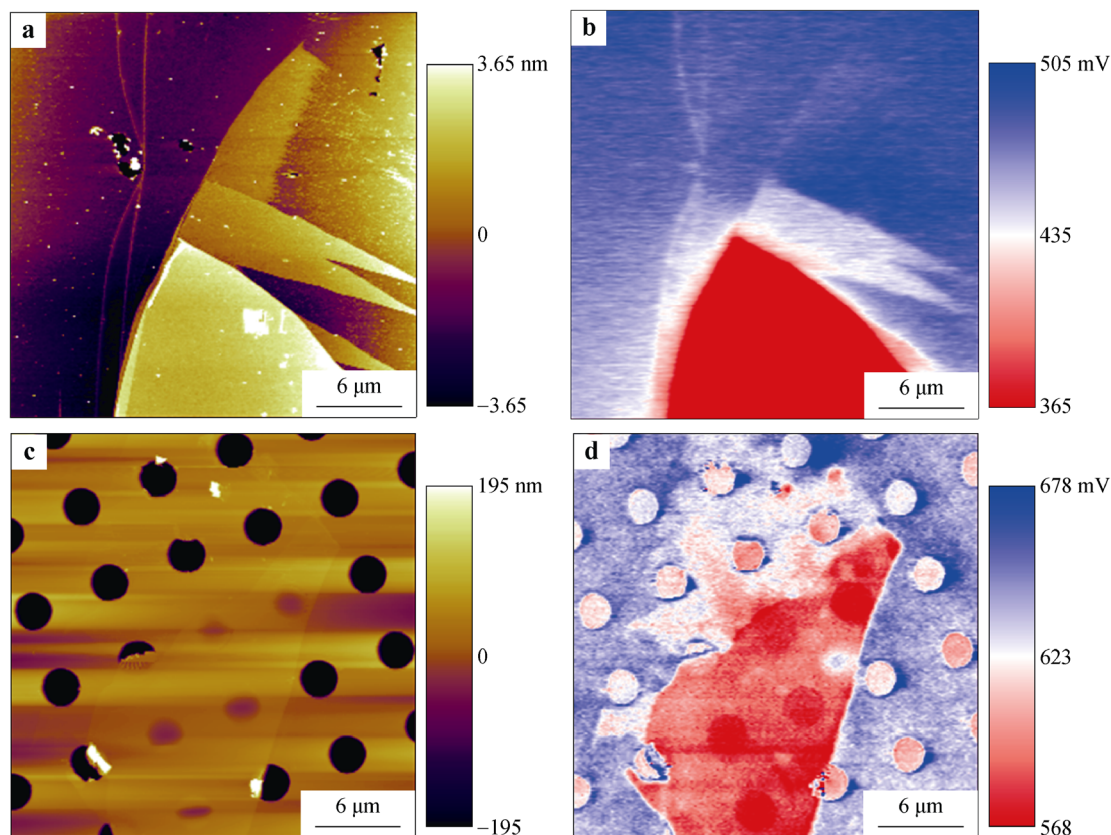

Fig. 2 Surface potential of few-layer InSe flakes: **a** topography and **b** surface potential images of supported InSe; **c** topography and **d** surface potential images of suspended InSe
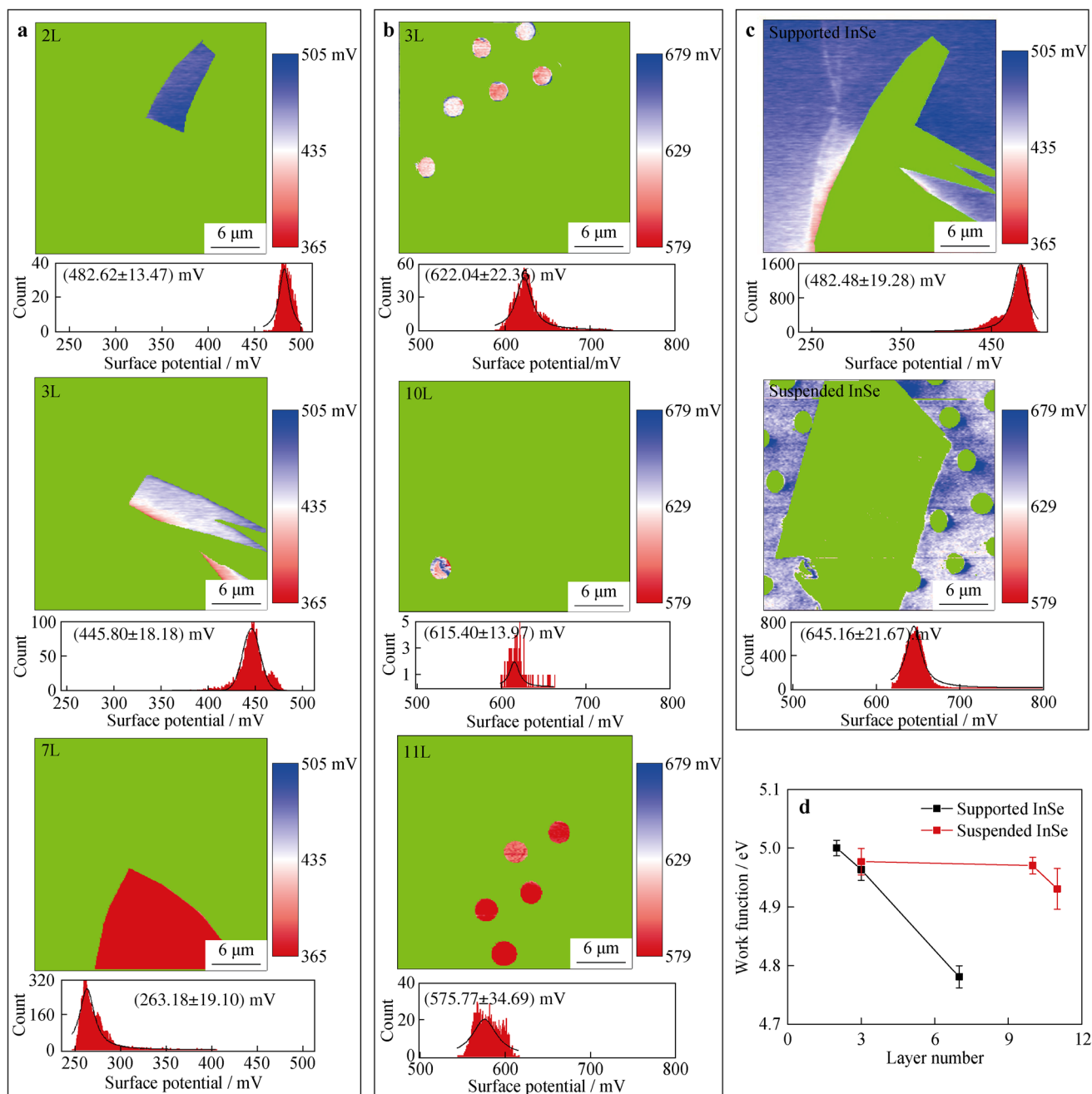
Fig. 3 Work function of few-layer InSe flakes: **a** surface potential maps and histograms of supported InSe for 2L, 3L and 7L, respectively; **b** surface potential maps and histograms of suspended InSe for 3L, 10L and 11L (L: layers), respectively; **c** surface potential maps and histograms of SiO$_2$ substrate for supported and suspended samples; **d** work function versus layer count of supported and suspended InSe

potential of InSe decreases monotonously with the increase in the layer count. For suspended InSe, the surface potential of InSe also decreases monotonously with the increase in the layer count, as shown in Fig. 2d.

To extract the exact surface potential of supported and suspended InSe, the surface potential maps in Fig. 2 were divided into several parts based on their layer counts, as shown in Fig. 3. Specifically, Fig. 3a shows 2L, 3L and 7L surface potential maps and histograms of supported InSe

which give corresponding surface potential values of (482.62 ± 13.47), (445.80 ± 18.18) and (263.18 ± 19.10) mV based on Gaussian fitting, respectively; Fig. 3b illustrates 3L, 10L and 11L surface potential maps and histograms of suspended InSe which give related surface potential values of (622.04 ± 22.36), (615.40 ± 13.97) and (575.77 ± 34.69) mV based on Gaussian fitting, respectively; Fig. 3c presents the surface potential maps and histograms of SiO$_2$ substrate of supported and
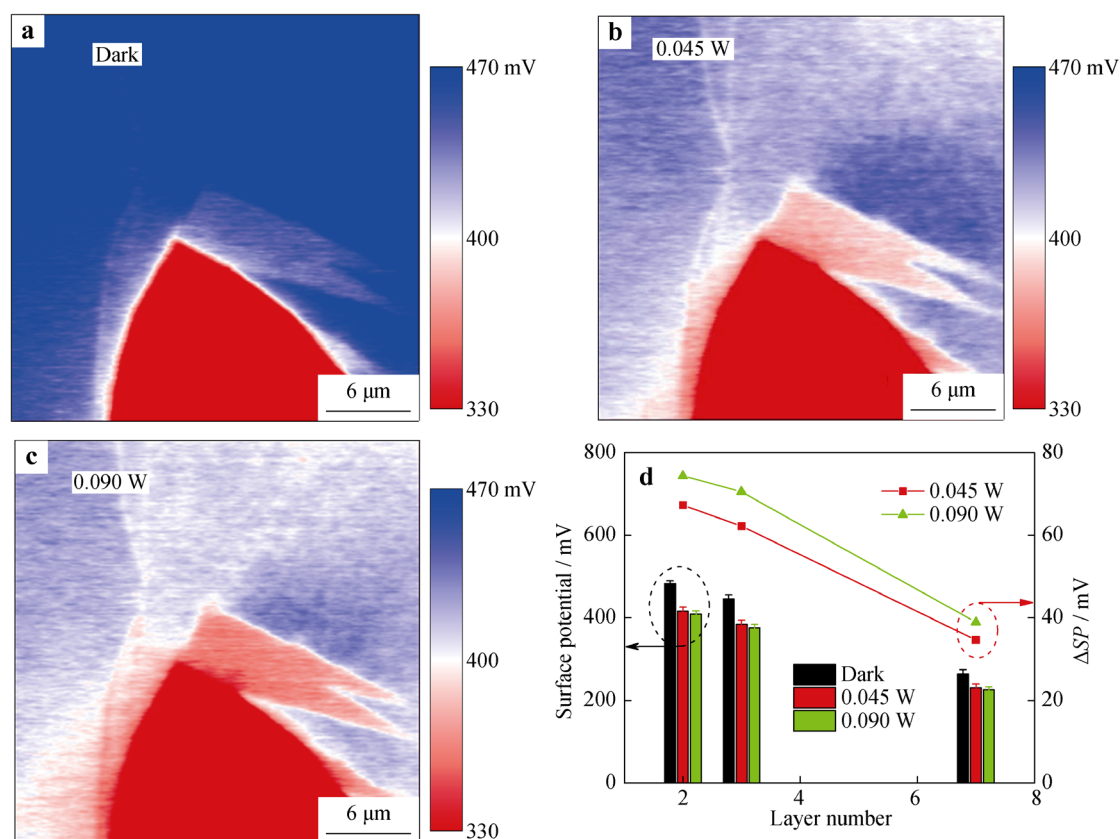
Fig. 4 Light-excited surface potential of supported InSe: **a** surface potential maps of InSe **a** in dark, under illumination with intensity of **b** 0.045 mW and **c** 0.09 mW; **d** surface potential (right, black) and ΔSP (left, red) between light and dark states of supported InSe versus its layer count for different light intensities

suspended samples which give correlated surface potential values of (482.48 ± 19.28) and (645.16 ± 21.67) mV based on Gaussian fitting, respectively. Based on Eq. (4) and the work function of SiO_2 (5.00 eV) [30], the work functions of tips for supported and suspended InSe samples can be deduced, separately, and the work functions of supported and suspended InSe can be determined. Detailedly, the work function of supported InSe drops from (5.00 ± 0.01) to (4.78 ± 0.02) eV when its thickness increases from 2L to 7L, and that of the suspended InSe decreases from (4.97 ± 0.02) to (4.93 ± 0.03) eV when its thickness increases from 3L to 11L, as shown in Fig. 3d. These results indicate that the work function of InSe decreases with the increase in the layer count of both supported and suspended InSe, which is consistent with DFT calculation [20].

3.3 Light-excited surface potential of a few-layer InSe

To explore the influence of light intensity on the surface potential of InSe, the supported InSe is illuminated by an integrated 405-nm (3.06 eV) laser with tunable power. The band gap of a few-layer InSe is ~ 1.40 eV [25], and thus,

the laser is expected to excite the electron from highest energy state in the valence band to the lowest energy state in the conduction band. And the work function and band gap of SiO_2 are around 5.00 and 9.00 eV, respectively [30]. The surface potential of InSe under light intensities of 0, 0.045 and 0.09 W was measured, as shown in Fig. 4a-c. The increased light intensity is accompanied by decreased surface potential. The surface potential of supported InSe also decreases with the increase in the layer count under illumination. Figure 4d shows the surface potential of InSe in dark, under 0.045 and 0.090 W illumination for different layer counts, and the surface potential shift between light and dark states ($\Delta SP = SP_{light} - SP_{dark}$) of multiple-layer InSe under 0.045 and 0.090 W illumination. For 2L InSe, the surface potential decreases from (482.62 ± 13.47) to (408.38 ± 8.01) mV when the light intensity increases from 0 to 0.090 W. For 3L and 7L InSe, surface potential decreases from (445.80 ± 18.18) to (375.49 ± 8.23) mV and from (263.18 ± 19.1) to (225.67 ± 7.26) mV, respectively, when the light intensity increases from 0 to 0.090 W. It is evident that light excites electrons, resulting in decreased surface potential, and the amount of electrons excited is correlated with light intensity. Finally, ΔSP

between light and dark states decreases from 67.20 to 33.20 mV for 0.045 W light intensity and from 74.20 to 37.50 mV for 0.090 W light intensity with layer count increasing from 2L to 7L, as shown in Fig. 4d, which suggests that the influence of light illumination decreases with the increase in the layer count of supported InSe.

4 Conclusion

By investigating the exfoliated few-layer InSe deposited on Si/SiO$_2$ with 300-nm-thick thermal oxide and Si/SiO$_2$ with 300-nm-thick thermal oxide and prefabricated micro-wells with 3 μm in diameter, the surface potential of few-layer InSe flakes was measured via KPFM integrated with 405-nm (3.06 eV) laser. Based on work function of SiO$_2$, the work function of supported and suspended InSe are determined which drops from (5.0 ± 0.01) to (4.78 ± 0.02) eV when its thickness increases from 2L to 7L, and that of the suspended InSe decreases from (4.97 ± 0.02) to (4.93 ± 0.03) eV when its thickness increases from 3L to 11L. Conclusively, the work function of InSe decreases with the increase in its layer count of both suspended and supported InSe, and 2L supported InSe has work function very close to SiO$_2$. By introducing laser illumination, the surface potential and the surface potential shift (ΔSP) between light and dark states of supported InSe were measured and deduced, respectively. These results show that the surface potential of supported InSe decreases with the increase in the light intensity and also decreases with the increase in the layer count. It is evident that light excites electrons, resulting in decreased surface potential, and the amount of electrons excited correlates with light intensity. And, ΔSP between light and dark states decreases with the increase in the layer count, suggesting that the influence of light illumination decreases with the increase in the layer count of few-layer InSe flakes.

References

[1] Xu M, Liang T, Shi M, Chen H. Graphene-like two-dimensional materials. Chem Rev. 2013;113(5):3766.

[2] Huang W, Gan L, Li H, Ma Y, Zhai T. 2D layered group IIIA metal chalcogenides: synthesis, properties and applications in electronics and optoelectronics. Cryst Eng Commun. 2016; 18(22):3968.

[3] Ferrari AC, Bonaccorso F, Fal'ko V, Novoselov KS, Roche S, Boggild P, Borini S, Koppens FH, Palermo V, Pugno N, Garrido JA, Sordan R, Bianco A, Ballerini L, Prato M, Lidorikis E, Kivioja J, Marinelli C, Ryhanen T, Morpurgo A, Coleman JN, Nicolosi V, Colombo L, Fert A, Garcia-Hernandez M, Bachtold A, Schneider GF, Guinea F, Dekker C, Barbone M, Sun Z, Galiotis C, Grigorenko AN, Konstantatos G, Kis A, Katsnelson M, Vandersypen L, Loiseau A, Morandi V, Neumaier D, Treossi E, Pellegrini V, Polini M, Tredicucci A, Williams GM, Hong BH, Ahn JH, Kim JM, Zirath H, van Wees BJ, van der Zant H, Occhipinti L, Di Matteo A, Kinloch IA, Seyller T, Quesnel E, Feng X, Teo K, Rupesinghe N, Hakonen P, Neil SR, Tannock Q, Lofwander T, Kinaret J. Science and technology roadmap for graphene, related two-dimensional crystals, and hybrid systems. Nanoscale. 2015;7(11):4598.

[4] Zhang Y, Tan YW, Stormer HL, Kim P. Experimental observation of the quantum Hall effect and Berry's phase in graphene. Nature. 2005;438(7065):201.

[5] Li T, Liu H, Shi P, Zhang Q. Recent progress in carbon/lithium metal composite anode for safe lithium metal batteries. Rare Met. 2018;37(6):449.

[6] Liu Y, Pharr M, Salvatore GA. Lab-on-skin: a review of flexible and stretchable electronics for wearable health monitoring. ACS Nano. 2017;11(10):9614.

[7] Novoselov KS, Geim AK, Morozov SV, Jiang D, Zhang Y, Dubonos SV, Grigorieva IV, Firsov A. Electric field effect in atomically thin carbon films. Science. 2004;306(5696):666.

[8] Dean CR, Young AF, Meric I, Lee C, Wang L, Sorgenfrei S, Watanabe K, Taniguchi T, Kim P, Shepard KL. Boron nitride substrates for high-quality graphene electronics. Nat Nanotechnol. 2010;5(10):722.

[9] Wang L, Meric I, Huang PY, Gao Q, Gao Y, Tran H, Taniguchi T, Watanabe K, Campos LM, Muller DA. One-dimensional electrical contact to a two-dimensional material. Science. 2013; 342(6158):614.

[10] Wang FK, Zhai TY. Towards scalable van der Waals heterostructure arrays. Rare Met. 2020;39(4):327.

[11] Peng Q, Xiong R, Sa B, Zhou J, Wen C, Wu B, Anpo M, Sun Z. Computational mining of photocatalysts for water splitting hydrogen production: two-dimensional InSe-family monolayers. Catal Sci Technol. 2017;7(13):2744.

[12] Bandurin DA, Tyurnina AV, Yu GL, Mishchenko A, Zolyomi V, Morozov SV, Kumar RK, Gorbachev RV, Kudrynskyi ZR, Pezzini S, Kovalyuk ZD, Zeitler U, Novoselov KS, Patane A, Eaves L, Grigorieva IV, Fal'ko VI, Geim AK, Cao Y. High electron mobility, quantum Hall effect and anomalous optical response in atomically thin InSe. Nat Nanotechnol. 2017;12(3): 223.

[13] Li Y, Yu C, Gan Y, Kong Y, Jiang P, Zou D, Li P, Yu X, Wu R, Zhao H, Gao CF, Li J. Elastic properties and intrinsic strength of two-dimensional InSe flakes. Nanotechnology. 2019;30(33): 335703.

[14] Cao R, Wang HD, Guo ZN, Sang DK, Zhang LY, Xiao QL, Zhang YP, Fan DY, Li JQ, Zhang H. Black phosphorous/indium selenide photoconductive detector for visible andnear-infrared light with high sensitivity. Adv Opt Mater. 2019;7(12):1900020.

[15] Lu HH, Shi CS, Zhao NQ, Liu EZ, He CN, He F. Carbon and few-layer MoS$_2$ nanosheets co-modified TiO$_2$ nanosheets with enhanced electrochemical properties for lithium storage. Rare Met. 2017;37(2):107.

[16] Li Y, Xu CY, Zhen L. Surface potential and interlayer screening effects of few-layer MoS$_2$ nanoflakes. Appl Phys Lett. 2013; 102(14):143110.

[17] Kim JH, Lee J, Kim JH, Hwang CC, Lee C, Park JY. Work

function variation of MoS_2 atomic layers grown with chemical vapor deposition: the effects of thickness and the adsorption of water/oxygen molecules. Appl Phys Lett. 2015;106(25):251606.

[18] Li F, Qi J, Xu M, Xiao J, Xu Y, Zhang X, Liu S, Zhang Y. Layer dependence and light tuning surface potential of 2D MoS_2 on various substrates. Small. 2017;13(14):1603103.

[19] Tamulewicz M, Kutrowska-Girzycka J, Gajewski K, Serafinczuk J, Sierakowski A, Jadczak J, Bryja L, Gotszalk TP. Layer number dependence of the work function and optical properties of single and few layers MoS_2: effect of substrate. Nanotechnology. 2019;30(24):245708.

[20] Sang DK, Wang H, Qiu M, Cao R, Guo Z, Zhao J, Li Y, Xiao Q, Fan D, Zhang H. Two dimensional beta-InSe with layer-dependent properties: band alignment, work function and optical properties. Nanomaterials (Basel). 2019;9(1):82.

[21] Li J, Huang B, Nasr Esfahani E, Wei L, Yao J, Zhao J, Chen W. Touching is believing: interrogating halide perovskite solar cells at the nanoscale via scanning probe microscopy. NPJ Quantum Mater. 2017;2(1):56.

[22] Melitz W, Shen J, Kummel AC, Lee S. Kelvin probe force microscopy and its application. Surf Sci Rep. 2011;66(1):1.

[23] Li Y, Yu C, Gan Y, Jiang P, Yu J, Ou Y, Zou DF, Huang C, Wang J, Jia T, Luo Q, Yu XF, Zhao H, Gao CF, Li J. Mapping the elastic properties of two-dimensional MoS_2 via bimodal atomic force microscopy and finite element simulation. NPJ Comput Mater. 2018;4:49.

[24] Li Y, Kong Y, Peng J, Yu C, Li Z, Li P, Liu Y, Gao CF, Wu R. Rapid identification of two-dimensional materials via machine learning assisted optic microscopy. J Materiomics. 2019;5(3): 413.

[25] Lei S, Ge L, Najmaei S, George A, Kappera R, Lou J, Chhowalla M, Yamaguchi H, Gupta G, Vajtai R. Evolution of the electronic band structure and efficient photo-detection in atomic layers of InSe. ACS Nano. 2014;8(2):1263.

[26] Nataly Chen Q, Liu Y, Liu Y, Xie S, Cao G, Li J. Delineating local electromigration for nanoscale probing of lithium ion intercalation and extraction by electrochemical strain microscopy. Appl Phys Lett. 2012;101(6):063901.

[27] Brotons-Gisbert M, Sánchez-Royo JF, Martínez-Pastor JP. Thickness identification of atomically thin InSe nanoflakes on SiO_2/Si substrates by optical contrast analysis. Appl Surf Sci. 2015;354:453.

[28] Sánchez-Royo JF, Muñoz-Matutano G, Brotons-Gisbert M, Martínez-Pastor JP, Segura A, Cantarero A, Mata R, Canet-Ferrer J, Tobias G, Canadell E, Marqués-Hueso J, Gerardot BD. Electronic structure, optical properties, and lattice dynamics in atomically thin indium selenide flakes. Nano Res. 2014;7(10):1556.

[29] Nan H, Guo S, Cai S, Chen Z, Zafar A, Zhang X, Gu X, Xiao S, Ni Z. Producing air-stable InSe nanosheet through mild oxygen plasma treatment. Semicond Sci Technol. 2018;33(7):074002.

[30] Vella E, Messina F, Cannas M, Boscaino R. Unraveling exciton dynamics in amorphous silicon dioxide: interpretation of the optical features from 8 to 11 eV. Phys Rev B. 2011;83(17): 174201.